

High-energy meson-baryon scattering in a quark model

Ramesh Chand

Department of Physics, Himachal Pradesh University, Simla, India

(Received 30 July 1973)

In a broken-SU(3) quark model, high-energy scattering processes of the type $PN \rightarrow P'B$ are investigated in the crossed t channel. We assume that the physical baryon octet contained in the direct product $\underline{3} \otimes \underline{3} \otimes \underline{3}$ is given by $\underline{8}$ (physical) = $\underline{8}' \cos \theta + \underline{8} \sin \theta$, where the baryon octets $\underline{8}$ and $\underline{8}'$ arise from $\underline{3} \otimes \underline{3}$ and $\underline{3} \otimes \underline{6}$, respectively. It is found that the value $\theta \simeq 20^\circ$, which explains reasonably well the available data on (a) high-energy photoproduction of mesons and (b) antiproton-nucleon annihilations into two mesons, also explains reasonably well the recently compiled data on meson-baryon scattering.

I. INTRODUCTION

In an earlier paper, we discussed in our simple quark model a few of the important features of high-energy meson-baryon scattering.¹ In particular, we compared our calculations with the available data on the ratios of the quantities² $\sigma_t(K^-p) - \sigma_t(K^+p)$, $\sigma_t(\pi^-p) - \sigma_t(\pi^+p)$, and $\sigma_t(K^-n) - \sigma_t(K^+n)$. It was found that $\theta \simeq 20^\circ$ explains reasonably well the available data on these ratios; θ is the mixing angle which defines the physical baryon octet in terms of the octets $\underline{8}$ and $\underline{8}'$. In this paper, we shall present our detailed calculations on high-energy meson-baryon scattering, and compare them with the available data.

The high-energy reactions of interest to us in this paper are

$$P + N \rightarrow P' + B, \quad (1)$$

where P and P' stand for the pseudoscalar meson, N stands for the proton p or the neutron n , and B stands for the baryon (singlet, octet, and the decuplet). At the present time, reasonable amounts of data are available on these processes,³ thereby allowing a good test for our quark-model calculations.

There exist in the published literature many versions of the quark model and, quite often, the predictions of these models are in disagreement with the experimental data.^{2,4,5} (Here, we shall list only a few of the published papers on this subject.) However, we have found that our broken-SU(3) quark model explains reasonably well the available data on (a) high-energy meson-baryon scattering,^{1,6} (b) high-energy photoproduction of mesons,⁷ and (c) antiproton-nucleon annihilations at rest.⁸

As in other quark models, the pseudoscalar-meson octet P_i^j is a composite of $Q\bar{Q}$. The baryon states are contained in the direct product

$$\begin{aligned} \underline{3} \otimes \underline{3} \otimes \underline{3} &= (\underline{3} \otimes \underline{\bar{3}}) \oplus (\underline{3} \otimes \underline{6}) \\ &= \underline{8} \oplus \underline{1} \oplus \underline{10} \oplus \underline{8}'. \end{aligned} \quad (2)$$

We shall write the baryon wave functions in terms of the third-rank tensor

$$B_{ijk} = Q_i Q_j Q_k. \quad (3)$$

In this paper, we use the notation of Okubo where the subscript refers to the quark and the superscript refers to the antiquark.⁹ Our meson and baryon wave functions are listed in the appendix of Ref. 10. (The baryon singlet state S in Ref. 10 is to be identified with the 1405-MeV Y_0^* resonance.)

In our quark model, there are two baryon octets present whereas, experimentally, there is only one baryon octet available. Therefore, we choose our physical baryon octet as

$$\underline{8}(\text{physical}) = \underline{8}' \cos \theta + \underline{8} \sin \theta, \quad (4)$$

and assume the value of the mixing angle θ to be 20° . In other words, we are interested in finding out whether or not $\theta = 20^\circ$ can explain the available data on high-energy meson-baryon scattering. This value of θ is dictated to us by the comparison of our quark-model calculations with the available data on various particle reactions.^{1,6-8}

It must be mentioned that corresponding to our $\underline{8}(\text{physical})$ there exists another baryon octet $\underline{8}(\text{orthogonal})$,

$$\underline{8}(\text{orthogonal}) = -\underline{8}' \sin \theta + \underline{8} \cos \theta. \quad (5)$$

However, owing to the fact that experimentally there is only one baryon octet available, we assume that at energies of interest to us $\underline{8}(\text{orthogonal})$ is not populated and hence we assume zero value for the coefficient multiplying it. [A similar situation exists in SU(6) symmetry, where we assume that the available baryon states are contained *only* in the $\underline{56}$ representation of $\underline{6} \otimes \underline{6} \otimes \underline{6}$.]

In Sec. II, we calculate the matrix elements for meson-baryon scattering. A number of sum rules are obtained in Sec. III. Our results are compared with the available data in Sec. IV.

II. CALCULATIONS

In calculating the matrix elements for high-energy $PN \rightarrow P'B$ reactions, we shall assume the validity of (a) the impulse approximation, and (b) time-reversal invariance. Also, at energies of interest to us, the angular distributions for these processes are strongly peaked in the forward direction.³ This implies the dominance of the crossed t -channel effects, with the basic interaction being governed by the exchange of singlet and octet objects only ($3 \otimes \bar{3} = 8 \oplus 1$). Under these assumptions, our interaction is represented by Fig. 1 and, corresponding to this diagram, the t -channel effective Lagrangian can be written as

$$L_{\text{eff}}(t) = A_1^{(m)} \chi_c^c P_{sd}^d + 6\hat{b}[\chi_d^c - \frac{1}{3}\delta_c^d \chi_e^e] \\ \times [A_s^{(m)}(P_{sc}^d - \frac{1}{3}\delta_c^d P_{sf}^f) + A_a^{(m)} P_{ac}^d], \quad (6)$$

where

$$\chi_d^c = \bar{B}_{abc} B_{abd}, \quad (6a)$$

$$P_s = \frac{1}{2}(\bar{P}P + P\bar{P}), \quad (6b)$$

$$P_a = \frac{1}{2}(\bar{P}P - P\bar{P}). \quad (6c)$$

The overbar refers to the incoming state, and P refers to the pseudoscalar-meson octet. In expression (6), the numerical factor of 6 is introduced for convenience.

The over-all complex amplitudes, the singlet exchange amplitude $A_1^{(m)}$, and the octet exchange amplitudes $A_s^{(m)}$ and $A_a^{(m)}$ are the integrals over the space-time variables and contain all the spin and kinematic dependences. The spin coupling is taken into account by the superscript m ; $m=1, 8$, or 10 , depending upon whether the final baryons belong to the SU(3) singlet, or octet, or the decuplet. Clearly, $A_1^{(1)} = A_1^{(10)} = 0$ because $8 \otimes 1$ and $8 \otimes 10$ do not couple to the SU(3) singlet exchanged particle. It may be mentioned that the use of R invariance will reduce the number of allowed amplitudes $A^{(m)}$. However, since R invariance does not seem to be a good symmetry in particle physics, we shall not use it in this paper.¹¹

The SU(3)-symmetry-breaking effects are introduced into our calculations by treating the exchange of strange quark λ_0 differently from the exchange of nonstrange quarks p_0 and n_0 . This is accomplished by the inclusion of the symmetry-breaking operator \hat{b} , defined as

$$\hat{b} = 1, \quad \text{for } p_0 \text{ and } n_0 \text{ exchanges,} \\ = b, \quad \text{for } \lambda_0 \text{ exchange.} \quad (7)$$

The value of b is to be understood in the limit

$$b = \lim_{s \rightarrow \infty} b(s), \quad (8)$$

where s is the square of the c.m. energy.

Now, in order to calculate the $PN \rightarrow P'B$ matrix elements, we use Eqs. (4) and (7) in (6) together with the values of P_j^i and B_{abc} from the appendix of Ref. 10. Then dropping the word "physical" from the baryon octet states, our matrix elements so obtained are given in Appendix A. (We have written down only the matrix elements for incident charged meson.) In these expressions, the mixing parameter a is defined by the relation

$$a = \cos 2\theta - \sqrt{3} \sin 2\theta \\ = -0.3473 \quad \text{for } \theta = 20^\circ. \quad (9)$$

First of all, we notice that in our particular quark model, because of using the impulse approximation, the matrix elements are zero for all those reactions which involve either double charge exchange or double strangeness exchange for the baryon (such as the production of Σ^- and Ξ hyperons). In higher-order calculations, these matrix elements are certainly nonzero.⁶ However, we find that at high energies of interest to us, the experimental values of the cross sections involving $\Delta Q=2$ and/or $\Delta S=2$ transitions are negligible³ as compared with the cross sections involving $\Delta Q=0, 1$ and $\Delta S=0, 1$ for the baryon. This, in a sense, justifies the correctness of our approximation.

It is important to compare our calculations with the SU(3) calculations of Salin.¹² Except for the symmetry-breaking parameter b , we find that

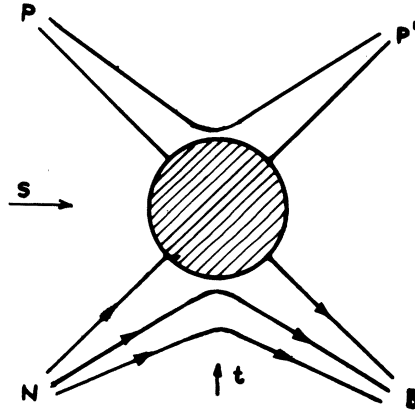


FIG. 1. Typical diagram for the scattering of pseudo-scalar mesons with baryons in a quark model, using the impulse approximation.

our mixing parameter a is related to the parameter α [$\alpha = d/(f+d)$] by the relation

$$a = 4\alpha/(3 - 4\alpha). \quad (10)$$

For $\theta = 20^\circ$ ($a = -0.3473$), we get

$$\alpha = -0.40.$$

It may be mentioned that Barger and Olsson¹³ obtain $\alpha = -1$, which corresponds to $\theta = 23.3^\circ$, whereas Salin¹² in his SU(3) + Regge-pole model calculations obtains $\alpha = -0.1$, which corresponds to $\theta = 16.7^\circ$. The discrepancy in these values of θ and ours is due to the fact that we use more recent values of the cross sections, and also because we treat the exchange of strange quarks differently from the exchange of nonstrange quarks ($b \neq 1$).

It is worthwhile to point out that in relation (10) the parameter a enters through the octet-baryon wave functions, whereas the parameter α in the SU(3) calculations enters through the f and d couplings in the effective Lagrangian. Of course, in the SU(3) calculations, one assumes

$$\begin{aligned} \alpha &= \alpha_1 \text{ for } 1^- \text{ octet-vector-meson exchange} \\ &= \alpha_2 \text{ for } 2^+ \text{ octet-tensor-meson exchange.} \end{aligned} \quad (11)$$

Experimentally, $\alpha_1 \simeq \alpha_2$.

In order to compare our calculations with the available experimental data, we first note the relation between the measured cross sections $\sigma(PN \rightarrow P'B)$ and the rate

$$R(PN \rightarrow P'B) \equiv |\langle P'B | PN \rangle|^2$$

given by Meshkov *et al.*¹⁴:

$$R = s p_i / p_f, \quad (12)$$

where s , p_i , and p_f denote in the c.m. system the total energy squared, the incident momentum, and the final momentum, respectively. However, in the sum rules given in Sec. III the kinematical factors are not very important at energies of interest to us ($p_L \geq 5$ GeV/c, p_L being the incident laboratory momentum of the pseudoscalar meson). We may mention here that the total cross section σ_t is obtained from the elastic scattering amplitude by using the optical theorem.

Unfortunately, owing to the inadequacy of the experimental data, it is not possible to determine the unknown amplitudes $A^{(m)}$, and hence we cannot predict the individual rates.

III. SUM RULES

Here, we shall obtain, among the various matrix elements, several relations, which are independent of the seven unknown amplitudes $A_1^{(8)}$, $A_s^{(1)}$, $A_s^{(8)}$,

$A_s^{(10)}$, $A_a^{(1)}$, $A_a^{(8)}$, and $A_a^{(10)}$. Since we want to see whether or not $\theta = 20^\circ$, which corresponds to $a = -0.3473$, explains the available data, we shall assume a to be known. Also, we shall take b to be a parameter whose value is to be determined. Then, since there are 63 matrix elements described in terms of seven unknown $A^{(m)}$, this gives us 56 relations listed in Appendix B.

From Appendix B, it is trivial to see that those relations which involve only particles belonging to the same isospin multiplets on both sides are a consequence of charge independence. This is, of course, to be expected because charge independence is a built-in feature of our quark model. Also, if we ignore the SU(3)-symmetry-breaking effects, i.e., take $b = 1$, then except for relations (B24), (B25), and (B26), others follow from the group SU(3)/Z(3). (This can be easily seen by comparing these sum rules with the ones given in Ref. 15.) Thus, in a sense, relations (B24), (B25), and (B26) are the specific predictions of our model. Of course, the inclusion of SU(3)-symmetry-breaking effects results in considerable improvements.

With the available data at the present time, the sum rule (B47) provides the best determination of b . Ignoring the phase-space correction factor which amounts to an effect of less than 1% at 5.5 GeV/c, we have

$$b = \left(\frac{\sigma(\pi^+ p \rightarrow K^+ Y_1^{*+})}{\sigma(K^- p \rightarrow K^- \Delta^+)} \right)^{1/2}. \quad (13)$$

The experimental data at $p_L = 5.5$ GeV/c give³

$$b \simeq 0.4. \quad (14)$$

On the basis of our earlier calculations,¹⁶ we believe that this value of b will decrease with the increase of p_L , and in the asymptotic limit [$b \equiv \lim_{s \rightarrow \infty} b(s)$] we hope to have $b \simeq 0.2$. It should of course be kept in mind that our t -channel calculations are expected to be good at high energies.

IV. DISCUSSION

In this section, we shall compare our calculations with the available high-energy data on $PN \rightarrow P'B$ reactions. First of all, we note that all those sum rules which are a consequence of charge independence are satisfied within the statistical fluctuations of the experimental data.³ (Hence, it will be unprofitable to discuss such sum rules any further.) The experimental data which we shall use in this paper are the compilations given in Ref. 3.

Relations (B14) and (B16) give

$$R(K^-n \rightarrow \pi^- \Lambda) = \frac{1}{2} |[R(K^-p \rightarrow \pi^0 \Lambda)]^{1/2} - [3R(K^-p \rightarrow \eta \Lambda)]^{1/2} \exp(i\phi_1)|^2, \quad (15)$$

where

$$\phi_1 = \arg\langle \eta \Lambda | K^- p \rangle - \arg\langle \pi^0 \Lambda | K^- p \rangle.$$

The data at 3 GeV/c are consistent with expression (15) for $\phi_1 \approx \pi$. (Data are not available to test this sum rule for $p_L > 3$ GeV/c.)

Sum rules (B34) and (B38) lead to

$$R(\pi^+ n \rightarrow \pi^+ \Delta^0) = |[R(K^+ p \rightarrow K^+ \Delta^+)]^{1/2} - [R(K^- p \rightarrow K^- \Delta^+)]^{1/2} \exp(i\phi_2)|^2, \quad (16)$$

where

$$\phi_2 = \arg\langle K^- \Delta^+ | K^- p \rangle - \arg\langle K^+ \Delta^+ | K^+ p \rangle.$$

For $\phi_2 \approx \pi$, the available data at 3 GeV/c agree with relation (16).

Using the optical theorem, the sum rules (B24) and (B25) can be written as

$$(2-a)[\sigma_t(K^-p) - \sigma_t(K^+p)] = (4+a)[\sigma_t(K^-n) - \sigma_t(K^+n)], \quad (17)$$

$$2(1+a)[\sigma_t(K^-p) - \sigma_t(K^+p)] = (4+a)[\sigma_t(\pi^-p) - \sigma_t(\pi^+p)]. \quad (18)$$

It is important to mention here that we shall test these and other relations at the same value of the laboratory momentum p_L . Since at high energies the c.m. momentum $p \propto \sqrt{p_L}$, it follows that at high energies of interest to us the kinematical factors cancel out in writing relations (17) and (18).

As mentioned earlier, one of our main aims here is to test whether or not $\theta = 20^\circ$ would explain the available high-energy data on meson-baryon scattering. Therefore, in expressions (17) and (18), we shall use $\theta = 20^\circ$. In Tables I and II, we present the experimental data to test relations (17) and (18) for p_L in the range of 6–50 GeV/c.

TABLE I. Experimental values of $(2-a)[\sigma_t(K^-p) - \sigma_t(K^+p)]$ and $(4+a)[\sigma_t(K^-n) - \sigma_t(K^+n)]$ for $\theta = 20^\circ$ ($a = -0.3473$) as a function of incident meson laboratory momentum p_L . These values were computed to test sum rule (17).

p_L (GeV/c)	$(2-a)[\sigma_t(K^-p) - \sigma_t(K^+p)]$ for $\theta = 20^\circ$ (mb)	$(4+a)[\sigma_t(K^-n) - \sigma_t(K^+n)]$ for $\theta = 20^\circ$ (mb)
6	16.4 ± 1.0	16.1 ± 2.9
8	14.8 ± 0.7	7.7 ± 2.9
10	12.2 ± 0.7	11.3 ± 2.9
12	10.1 ± 0.7	9.5 ± 2.9
14	9.6 ± 0.7	9.5 ± 2.9
16	10.1 ± 1.2	10.6 ± 3.6
18	9.2 ± 2.1	9.9 ± 5.5
20	8.9 ± 1.9	5.8 ± 3.9
30	8.4 ± 1.1	8.8 ± 2.6
40	5.7 ± 0.7	4.6 ± 2.6
50	4.8 ± 0.5	6.8 ± 2.9

From Table I, we notice that within the uncertainties of the experimental data, the sum rule (17) is reasonably well satisfied except at $p_L = 8$ GeV/c. This discrepancy is perhaps due to the fact that the Kn data, which are extracted from the Kd measurements, are not very accurate.

As far as relation (18) is concerned, within the uncertainties of the experimental measurements, it is reasonably satisfied for p_L in the range of 6–30 GeV/c. However, if we assume that the correct estimate of experimental uncertainties is given by three standard deviations, then this relation is all right even for $p_L = 40$ and 50 GeV/c. (Fermi always used to say that the correct estimate of the errors in experimental measurements should be taken as 3σ and *not* 1σ .)

It may be mentioned that in SU(6) symmetry, one predicts²

$$\begin{aligned} \frac{1}{2}[\sigma_t(K^-p) - \sigma_t(K^+p)] &= \sigma_t(K^-n) - \sigma_t(K^+n) \\ &= \sigma_t(\pi^-p) - \sigma_t(\pi^+p), \end{aligned} \quad (19)$$

which corresponds to $a = 0$ ($\theta = 15^\circ$) in our case. Clearly, these SU(6) predictions are in disagreement with the available data.

Relation (B26), on using the optical theorem, leads to

TABLE II. Experimental values of $2(1+a)[\sigma_t(K^-p) - \sigma_t(K^+p)]$ and $(4+a)[\sigma_t(\pi^-p) - \sigma_t(\pi^+p)]$ for $\theta = 20^\circ$ ($a = -0.3473$) as a function of incident meson laboratory momentum p_L . These values were computed to test sum rule (18).

p_L (GeV/c)	$2(1+a)[\sigma_t(K^-p) - \sigma_t(K^+p)]$ for $\theta = 20^\circ$ (mb)	$(4+a)[\sigma_t(\pi^-p) - \sigma_t(\pi^+p)]$ for $\theta = 20^\circ$ (mb)
6	9.1 ± 0.5	8.4 ± 1.8
8	8.2 ± 0.4	8.8 ± 1.8 (1965 value)
		11.3 ± 7.3 (1969 value)
10	6.8 ± 0.4	6.2 ± 1.8
12	5.6 ± 0.4	6.2 ± 1.8
14	5.4 ± 0.4	5.5 ± 1.8
16	5.6 ± 0.7	6.2 ± 1.8
18	5.1 ± 1.2	5.5 ± 1.8
20	4.9 ± 1.0	7.7 ± 3.3
30	4.7 ± 0.7	5.3 ± 0.7
40	3.2 ± 0.4	4.7 ± 0.7
50	2.7 ± 0.3	4.3 ± 0.7

$$(2-a)[\sigma_t(\pi^-n) - \sigma_t(K^-n)] = (4+a)[\sigma_t(\pi^-p) - \sigma_t(K^-p)]. \quad (20)$$

This relation is valid provided we compare both sides at the same value of p_L and also provided p_L is large. Unfortunately, there are no data on $\sigma_t(\pi^-n)$ and $\sigma_t(K^-n)$ for $p_L < 20$ GeV/c. However, for p_L in the range of (20–50) GeV/c, data are available to test the sum rule (20). In Table III, we present the data as a function of p_L for two values of θ , viz. $\theta=20^\circ$ and $\theta=30^\circ$. From this table, we notice that at 20 GeV/c, relation (20) is satisfied within the uncertainties of the experimental measurements by both values of θ , namely $\theta=20^\circ$ and $\theta=30^\circ$. However, for $p_L > 20$ GeV/c the value $\theta=30^\circ$, which corresponds to $a=-1$, provides a much better fit to relation (20) than does $\theta=20^\circ$. However, the use of $\theta=30^\circ$ in expression (18) requires

$$\sigma_t(\pi^-p) = \sigma_t(\pi^+p) \quad \text{for } \theta=30^\circ, \quad (21)$$

which does not agree with the presently available data.³ It must of course be noted that the sum rule (18) is reasonably satisfied with $\theta=20^\circ$. We cannot rule out the possibility that the source of this discrepancy may lie in the presently compiled values of $\sigma_t(\pi^-n)$ and $\sigma_t(K^-n)$, which are obtained from the π^-d and K^-d measurements. It is, therefore, necessary that π^-n and K^-n total cross sections be measured very accurately because even a decrease of 5% in the present values of $\sigma_t(K^-n)$ will satisfy the sum rule (20) for $\theta=20^\circ$. Hence, with the presently available data, we cannot really say whether or not relation (20) is satisfied for $\theta=20^\circ$.

It is important to keep in mind that, in principle, θ can vary slightly with energy. This is quite apparent from relation (9), which connects a ($a \equiv \cos 2\theta - \sqrt{3} \sin 2\theta$) with α [$\alpha \equiv d/(f+d)$]. As one knows, in principle, α can be energy-dependent. Unfortunately, in the published literature, there is no paper which gives the energy dependence of α . At the present time, we are in the process of investigating the energy dependence of θ . However, our task is complicated by the fact that there are large uncertainties in the available experimental data.

It may be stated here that at first sight, it may be difficult to understand the possible energy dependence of θ , whereas it is quite easy to visualize the energy dependence of α because α enters in the effective Lagrangian through the d and f couplings. The energy dependence of θ can easily be understood in terms of a *gas model*. From relation (4), it is obvious that θ determines the relative proportions of “gases” $\underline{8}'$ and $\underline{8}$ in the observed “gas” $\underline{8}$ (physical). It is a well-known fact in chem-

istry that the relative proportions of the two “gases” $\underline{8}'$ and $\underline{8}$ constituting the “gas” $\underline{8}$ (physical) change with temperature.

It is worth pointing out here that in other quark models one obtains²

$$2[\sigma_t(K^-p) + \sigma_t(K^+p)] = [\sigma_t(\pi^-p) + \sigma_t(\pi^+p)] + [\sigma_t(K^-n) + \sigma_t(K^+n)]. \quad (22)$$

In our case, this equality holds only if $\theta=15^\circ$ and not 20° . As has been pointed out by Barger and Durand,² this relation is in sharp disagreement with the available experimental data.

An important quantity ϵ which is of interest to us is defined as

$$\epsilon = \sigma(K^-p \rightarrow \pi^0\Lambda) / \sigma_1, \quad (23)$$

where

$$\sigma_1 = \sigma(K^-p \rightarrow \pi^+\Sigma^-) + \sigma(K^-p \rightarrow \pi^-\Sigma^+) - 2\sigma(K^-p \rightarrow \pi^0\Sigma^0) + \sigma(K^-p \rightarrow \pi^0\Lambda).$$

ϵ gives the $K^-p \rightarrow \pi^0\Lambda$ cross section as a fraction of the total $I=1$, $K^-p \rightarrow \pi Y$ absorption cross section; Y stands for Σ or Λ hyperons. Using the matrix elements from Appendix A, we get

$$\epsilon = \left[1 + \frac{2}{3} \left(\frac{2-a}{2+a} \right)^2 \right]^{-1} = 0.43 \quad \text{for } \theta=20^\circ. \quad (24)$$

The experimental data at $p_L = 3$ GeV/c give

$$\epsilon = 0.44 \pm 0.1. \quad (25)$$

Hence, $\theta=20^\circ$ explains quite well the experimental value of ϵ at 3 GeV/c. Unfortunately, experimental data are not available to test the value of ϵ at higher energies.

It must be pointed out that the defects of other quark models, pointed out by Barger and Durand, are absent in our model.² Also, we note that Cabibbo *et al.*, in their Regge pole model, using quark-model vertices and trajectory degeneracy, obtain¹⁷

TABLE III. Experimental values of $(2-a)[\sigma_t(\pi^-n) - \sigma_t(K^-n)]$ and $(4+a)[\sigma_t(\pi^-p) - \sigma_t(K^-p)]$ for $\theta=20^\circ$ ($a=-0.3473$) and $\theta=30^\circ$ ($a=-1$) as a function of incident meson laboratory momentum p_L . These values were computed to test sum rule (20).

p_L (GeV/c)	$(2-a)[\sigma_t(\pi^-n) - \sigma_t(K^-n)]$ (mb)		$(4+a)[\sigma_t(\pi^-p) - \sigma_t(K^-p)]$ (mb)	
	$\theta=20^\circ$	$\theta=30^\circ$	$\theta=20^\circ$	$\theta=30^\circ$
20	9.9 ± 3.3	12.6 ± 4.2	16.0 ± 5.1	13.2 ± 4.2
25	9.4 ± 2.6	12.0 ± 3.3	14.6 ± 0.7	12.0 ± 0.6
30	8.2 ± 1.9	10.5 ± 2.4	12.8 ± 1.5	10.5 ± 1.2
40	8.7 ± 1.9	11.1 ± 2.4	14.2 ± 0.7	11.7 ± 0.6
45	7.3 ± 1.9	9.3 ± 2.4	14.2 ± 0.7	11.7 ± 0.6
50	8.2 ± 2.1	10.5 ± 2.7	14.2 ± 0.7	11.7 ± 0.6
55	6.6 ± 2.1	8.4 ± 3.9	14.9 ± 0.7	12.3 ± 0.6

$$\sigma_t(\pi^- p) = \sigma_t(K^- p), \quad (26a)$$

$$\sigma_t(\pi^+ p) = \sigma_t(K^- n). \quad (26b)$$

These equalities do not agree with our calculations nor with the available experimental data.³

Finally, owing to the lack of available data, the rest of the predictions of our quark model cannot be tested at the present time. However, it is our sincere hope that in the near future more data will become available on high-energy meson-baryon scattering.

V. CONCLUSIONS

In our simple broken-SU(3) quark model, under the assumption of additivity of the two-body quark amplitudes, most of our calculations are within the uncertainties of the experimental measurements in agreement with the available data. In order to test the sum rule (20) for $\theta = 20^\circ$ we need more accurate values of $\pi^- n$ and $K^- n$ total cross sections. Also, in order to test all the sum rules, given in Appendix B, it is necessary to have more, as well as accurate, data on the various $PN \rightarrow P'B$ reactions at high energies. This is also essential in order to determine whether or not θ has a slight energy dependence.

Since the SU(3)-symmetry-breaking parameter b is defined in the limit

$$\lim_{s \rightarrow \infty} b(s) = b,$$

we need the values of $\sigma(\pi^+ p \rightarrow K^+ Y_1^{*+})$ and $\sigma(K^- p \rightarrow K^- \Delta^+)$ at high energies (say for $p_L \geq 20$ GeV/c). On the basis of our quark-model calculations on high-energy photoproduction processes,¹⁶ we expect $b \approx 0.2$. Since at $p_L = 5.5$ GeV/c, we get $b(s) \approx 0.4$, it means that the value of the symmetry-breaking parameter is expected to decrease with increasing energy.¹⁸

Finally, we find that our quark-model calculations provide a considerably better fit to the high-energy meson-baryon scattering data than those of others using SU(6) symmetry, etc.^{2,4,5} Not only that, but our quark model also explains reasonably well the data on photoproduction and antiproton-nucleon reactions^{7,8} for $\theta \approx 20^\circ$. In fact, the objections raised by Barger and Durand against other quark-model predictions are absent in our calculations.²

APPENDIX A

Here, we give the matrix elements for physical baryons in high-energy meson-baryon scattering, using expressions (4) and (7) in (6), together with the values of the quark wave functions for pseudo-scalar mesons and the baryons from Ref. 10.

Then, in terms of the mixing parameter a defined

as

$$a = \cos 2\theta - \sqrt{3} \sin 2\theta \\ = -0.3473 \text{ for } \theta = 20^\circ,$$

these matrix elements are

$$\langle \pi^+ p | \pi^+ p \rangle = [A_1^{(8)} + A_s^{(8)}] + (1+a)A_a^{(8)}, \quad (A1)$$

$$\langle K^+ \Sigma^+ | \pi^+ p \rangle = -\frac{1}{2}b(2-a)[A_s^{(8)} - A_a^{(8)}], \quad (A2)$$

$$\langle \pi^+ \Delta^+ | \pi^+ p \rangle = -[2(2-a)]^{1/2}A_a^{(10)}, \quad (A3)$$

$$\langle \pi^0 \Delta^{++} | \pi^+ p \rangle = -[3(2-a)]^{1/2}A_a^{(10)}, \quad (A4)$$

$$\langle \eta \Delta^{++} | \pi^+ p \rangle = (2-a)^{1/2}A_s^{(10)}, \quad (A5)$$

$$\langle K^+ Y_1^{*+} | \pi^+ p \rangle = b[\frac{1}{2}(2-a)]^{1/2}[A_s^{(10)} - A_a^{(10)}], \quad (A6)$$

$$\langle \pi^- p | \pi^- p \rangle = [A_1^{(8)} + A_s^{(8)}] - (1+a)A_a^{(8)}, \quad (A7)$$

$$\langle \pi^0 n | \pi^- p \rangle = \sqrt{2}(1+a)A_a^{(8)}, \quad (A8)$$

$$\langle \eta n | \pi^- p \rangle = (\frac{3}{5})^{1/2}(1+a)A_s^{(8)}, \quad (A9)$$

$$\langle K^0 \Lambda | \pi^- p \rangle = -(\frac{3}{8})^{1/2}b(2+a)[A_s^{(8)} - A_a^{(8)}], \quad (A10)$$

$$\langle K^0 \Sigma^0 | \pi^- p \rangle = -(\frac{1}{6})^{1/2}b(2-a)[A_s^{(8)} - A_a^{(8)}], \quad (A11)$$

$$\langle \pi^- \Delta^+ | \pi^- p \rangle = [2(2-a)]^{1/2}A_a^{(10)}, \quad (A12)$$

$$\langle \pi^0 \Delta^0 | \pi^- p \rangle = -(2-a)^{1/2}A_a^{(10)}, \quad (A13)$$

$$\langle \eta \Delta^0 | \pi^- p \rangle = -[\frac{1}{3}(2-a)]^{1/2}A_s^{(10)}, \quad (A14)$$

$$\langle K^0 Y_1^{*0} | \pi^- p \rangle = -\frac{1}{2}b(2-a)^{1/2}[A_s^{(10)} - A_a^{(10)}], \quad (A15)$$

$$\langle K^0 Y_0^* | \pi^- p \rangle = \frac{1}{2}b[3(2+a)]^{1/2}[A_s^{(1)} - A_a^{(1)}], \quad (A16)$$

$$\langle K^+ p | K^+ p \rangle = [A_1^{(8)} + \frac{1}{2}aA_s^{(8)}] + \frac{1}{2}(4+a)A_a^{(8)}, \quad (A17)$$

$$\langle K^+ \Delta^+ | K^+ p \rangle = -[\frac{1}{2}(2-a)]^{1/2}[A_s^{(10)} + A_a^{(10)}], \quad (A18)$$

$$\langle K^0 \Delta^{++} | K^+ p \rangle = [\frac{3}{2}(2-a)]^{1/2}[A_s^{(10)} + A_a^{(10)}], \quad (A19)$$

$$\langle K^- p | K^- p \rangle = [A_1^{(8)} + \frac{1}{2}aA_s^{(8)}] - \frac{1}{2}(4+a)A_a^{(8)}, \quad (A20)$$

$$\langle \bar{K}^0 n | K^- p \rangle = (1+a)[A_s^{(8)} - A_a^{(8)}], \quad (A21)$$

$$\langle \pi^- \Sigma^+ | K^- p \rangle = -\frac{1}{2}b(2-a)[A_s^{(8)} + A_a^{(8)}], \quad (A22)$$

$$\langle \pi^0 \Lambda | K^- p \rangle = -(\sqrt{3}/4)b(2+a)[A_s^{(8)} + A_a^{(8)}], \quad (A23)$$

$$\langle \pi^0 \Sigma^0 | K^- p \rangle = -\frac{1}{4}b(2-a)[A_s^{(8)} + A_a^{(8)}], \quad (A24)$$

$$\langle \eta \Lambda | K^- p \rangle = \frac{1}{4}b(2+a)[A_s^{(8)} - 3A_a^{(8)}], \quad (A25)$$

$$\langle \eta \Sigma^0 | K^- p \rangle = (1/4\sqrt{3})b(2-a)[A_s^{(8)} - 3A_a^{(8)}], \quad (A26)$$

$$\langle K^- \Delta^+ | K^- p \rangle = -[\frac{1}{2}(2-a)]^{1/2}[A_s^{(10)} - A_a^{(10)}], \quad (A27)$$

$$\langle \bar{K}^0 \Delta^0 | K^- p \rangle = -[\frac{1}{2}(2-a)]^{1/2}[A_s^{(10)} - A_a^{(10)}], \quad (A28)$$

$$\langle \pi^- Y_1^{*+} | K^- p \rangle = b[\frac{1}{2}(2-a)]^{1/2}[A_s^{(10)} + A_a^{(10)}], \quad (A29)$$

$$\langle \pi^0 Y_1^{*0} | K^- p \rangle = -\frac{1}{2}b[\frac{1}{2}(2-a)]^{1/2}[A_s^{(10)} + A_a^{(10)}], \quad (A30)$$

$$\langle \eta Y_1^{*0} | K^- p \rangle = \frac{1}{2}b[\frac{1}{6}(2-a)]^{1/2}[A_s^{(10)} - 3A_a^{(10)}], \quad (A31)$$

$$\langle \pi^0 Y_0^* | K^- p \rangle = \frac{1}{2}b[\frac{3}{2}(2+a)]^{1/2}[A_s^{(1)} + A_a^{(1)}], \quad (A32)$$

$$\langle \eta Y_0^* | K^- p \rangle = \frac{1}{2} b \left[\frac{1}{2} (2+a) \right]^{1/2} [3A_a^{(1)} - A_s^{(1)}], \quad (\text{A39})$$

$$\langle \pi^+ n | \pi^+ n \rangle = [A_1^{(8)} + A_s^{(8)}] - (1+a)A_n^{(8)}, \quad (\text{A34})$$

$$\langle \pi^0 p | \pi^+ n \rangle = -\sqrt{2}(1+a)A_a^{(8)}, \quad (\text{A35})$$

$$\langle \eta p | \pi^+ n \rangle = \left(\frac{2}{3}\right)^{1/2} (1+a)A_s^{(8)}, \quad (\text{A36})$$

$$\langle K^+ \Lambda | \pi^+ n \rangle = -\left(\frac{3}{8}\right)^{1/2} b(2+a)[A_s^{(8)} - A_a^{(8)}], \quad (\text{A37})$$

$$\langle K^+ \Sigma^0 | \pi^+ n \rangle = \left(\frac{1}{8}\right)^{1/2} b(2-a)[A_s^{(8)} - A_a^{(8)}], \quad (\text{A38})$$

$$\langle \pi^+ \Delta^0 | \pi^+ n \rangle = -[2(2-a)]^{1/2} A_a^{(10)}, \quad (\text{A39})$$

$$\langle \pi^0 \Delta^+ | \pi^+ n \rangle = -(2-a)^{1/2} A_a^{(10)}, \quad (\text{A40})$$

$$\langle K^+ Y_1^{*0} | \pi^+ n \rangle = \frac{1}{2} b(2-a)^{1/2} [A_s^{(10)} - A_a^{(10)}], \quad (\text{A41})$$

$$\langle K^+ Y_0^* | \pi^+ n \rangle = \frac{1}{2} b[3(2+a)]^{1/2} [A_s^{(1)} - A_a^{(1)}], \quad (\text{A42})$$

$$\langle \pi^- n | \pi^- n \rangle = [A_1^{(8)} + A_s^{(8)}] + (1+a)A_n^{(8)}, \quad (\text{A43})$$

$$\langle K^0 \Sigma^- | \pi^- n \rangle = -\frac{1}{2} b(2-a)[A_s^{(8)} - A_a^{(8)}], \quad (\text{A44})$$

$$\langle \pi^- \Delta^0 | \pi^- n \rangle = [2(2-a)]^{1/2} A_a^{(10)}, \quad (\text{A45})$$

$$\langle \pi^0 \Delta^- | \pi^- n \rangle = -[3(2-a)]^{1/2} A_a^{(10)}, \quad (\text{A46})$$

$$\langle \eta \Delta^- | \pi^- n \rangle = -(2-a)^{1/2} A_s^{(10)}, \quad (\text{A47})$$

$$\langle K^0 Y_1^{*-} | \pi^- n \rangle = -b \left[\frac{1}{2} (2-a) \right]^{1/2} [A_s^{(10)} - A_a^{(10)}], \quad (\text{A48})$$

$$\langle K^+ n | K^+ n \rangle = [A_1^{(8)} - \frac{1}{2}(2+a)A_s^{(8)}] + \frac{1}{2}(2-a)A_n^{(8)}, \quad (\text{A49})$$

$$\langle K^0 p | K^+ n \rangle = (1+a)[A_s^{(8)} + A_a^{(8)}], \quad (\text{A50})$$

$$\langle K^+ \Delta^0 | K^+ n \rangle = -\left[\frac{1}{2}(2-a)\right]^{1/2} [A_s^{(10)} + A_a^{(10)}], \quad (\text{A51})$$

$$\langle K^0 \Delta^+ | K^+ n \rangle = \left[\frac{1}{2}(2-a)\right]^{1/2} [A_s^{(10)} + A_a^{(10)}], \quad (\text{A52})$$

$$\langle K^- n | K^- n \rangle = [A_1^{(8)} - \frac{1}{2}(2+a)A_s^{(8)}] - \frac{1}{2}(2-a)A_n^{(8)}, \quad (\text{A53})$$

$$\langle \pi^- \Lambda | K^- n \rangle = -\left(\frac{3}{8}\right)^{1/2} b(2+a)[A_s^{(8)} + A_a^{(8)}], \quad (\text{A54})$$

$$\langle \pi^- \Sigma^0 | K^- n \rangle = \left(\frac{1}{8}\right)^{1/2} b(2-a)[A_s^{(8)} + A_a^{(8)}], \quad (\text{A55})$$

$$\langle \pi^0 \Sigma^- | K^- n \rangle = -\left(\frac{1}{8}\right)^{1/2} b(2-a)[A_s^{(8)} + A_a^{(8)}], \quad (\text{A56})$$

$$\langle \eta \Sigma^- | K^- n \rangle = (1/2\sqrt{6})b(2-a)[A_s^{(8)} - 3A_a^{(8)}], \quad (\text{A57})$$

$$\langle K^- \Delta^0 | K^- n \rangle = -\left[\frac{1}{2}(2-a)\right]^{1/2} [A_s^{(10)} - A_a^{(10)}], \quad (\text{A58})$$

$$\langle \bar{K}^0 \Delta^- | K^- n \rangle = -\left[\frac{3}{2}(2-a)\right]^{1/2} [A_s^{(10)} - A_a^{(10)}], \quad (\text{A59})$$

$$\langle \pi^- Y_1^{*0} | K^- n \rangle = \frac{1}{2} b(2-a)^{1/2} [A_s^{(10)} + A_a^{(10)}], \quad (\text{A60})$$

$$\langle \pi^0 Y_1^{*-} | K^- n \rangle = -\frac{1}{2} b(2-a)^{1/2} [A_s^{(10)} + A_a^{(10)}], \quad (\text{A61})$$

$$\langle \eta Y_1^{*-} | K^- n \rangle = \frac{1}{2} b \left[\frac{1}{3} (2-a) \right]^{1/2} [A_s^{(10)} - 3A_a^{(10)}], \quad (\text{A62})$$

$$\langle \pi^- Y_0^* | K^- n \rangle = \frac{1}{2} b[3(2+a)]^{1/2} [A_s^{(1)} + A_a^{(1)}]. \quad (\text{A63})$$

APPENDIX B

Here, we list the 56 sum rules obtained by eliminating the seven unknown amplitudes $A_1^{(8)}$, $A_s^{(8)}$, $A_s^{(10)}$, $A_a^{(10)}$, $A_a^{(8)}$, $A_n^{(8)}$, and $A_n^{(10)}$ from the 63 matrix elements given in Appendix A. These relations are

$$\langle \pi^0 n | \pi^- p \rangle = -\langle \pi^0 p | \pi^+ n \rangle, \quad (\text{B1})$$

$$\langle \eta n | \pi^- p \rangle = \sqrt{3} \langle \eta p | \pi^+ n \rangle, \quad (\text{B2})$$

$$\langle \eta \Sigma^- | K^- n \rangle = \sqrt{2} \langle \eta \Sigma^0 | K^- p \rangle, \quad (\text{B3})$$

$$\langle \pi^+ p | \pi^+ p \rangle = \langle \pi^- n | \pi^- n \rangle, \quad (\text{B4})$$

$$\langle \pi^- p | \pi^- p \rangle = \langle \pi^+ n | \pi^+ n \rangle, \quad (\text{B5})$$

$$\langle \pi^- \Sigma^+ | K^- p \rangle = 2 \langle \pi^0 \Sigma^0 | K^- p \rangle = -\sqrt{2} \langle \pi^- \Sigma^0 | K^- n \rangle \quad (\text{B7})$$

$$= \sqrt{2} \langle \pi^0 \Sigma^- | K^- n \rangle, \quad (\text{B8})$$

$$\langle K^+ \Sigma^+ | \pi^+ p \rangle = \sqrt{2} \langle K^0 \Sigma^0 | \pi^- p \rangle \quad (\text{B9})$$

$$= -\sqrt{2} \langle K^+ \Sigma^0 | \pi^+ n \rangle \quad (\text{B10})$$

$$= \langle \pi^0 \Sigma^0 | K^- p \rangle - \sqrt{3} \langle \eta \Sigma^0 | K^- p \rangle \quad (\text{B11})$$

$$= b[\langle K^+ p | K^+ p \rangle - \langle \pi^+ p | \pi^+ p \rangle], \quad (\text{B12})$$

$$\langle K^+ \Lambda | \pi^+ n \rangle = \sqrt{2} \langle \pi^0 \Lambda | K^- p \rangle \quad (\text{B13})$$

$$= \langle \pi^- \Lambda | K^- n \rangle \quad (\text{B14})$$

$$= \langle K^0 \Lambda | \pi^- p \rangle \quad (\text{B15})$$

$$= (1/\sqrt{2})[\langle \pi^0 \Lambda | K^- p \rangle - \sqrt{3} \langle \eta \Lambda | K^- p \rangle], \quad (\text{B16})$$

$$\sqrt{2} \langle \bar{K}^0 n | K^- p \rangle = \sqrt{3} \langle \eta n | \pi^- p \rangle - \langle \pi^0 n | \pi^- p \rangle \quad (\text{B17})$$

$$= \sqrt{2} \langle K^0 p | K^+ n \rangle + 2 \langle \pi^0 p | \pi^+ n \rangle \quad (\text{B18})$$

$$= (1/b)[\langle K^0 \Sigma^0 | \pi^- p \rangle - \sqrt{3} \langle K^0 \Lambda | \pi^- p \rangle] \quad (\text{B19})$$

$$= \sqrt{2} [\langle K^- p | K^- p \rangle - \langle K^- n | K^- n \rangle], \quad (\text{B20})$$

$$\sqrt{2} \langle K^0 p | K^+ n \rangle = \langle \pi^0 n | \pi^- p \rangle + \sqrt{3} \langle \eta n | \pi^- p \rangle, \quad (\text{B21})$$

$$\sqrt{2} \langle \pi^0 n | \pi^- p \rangle = \langle \pi^+ p | \pi^+ p \rangle - \langle \pi^- p | \pi^- p \rangle, \quad (\text{B22})$$

$$\langle K^+ p | K^+ p \rangle = \langle K^+ n | K^+ n \rangle + \langle K^0 p | K^+ n \rangle, \quad (\text{B23})$$

$$(2-a)[\langle K^- p | K^- p \rangle - \langle K^+ p | K^+ p \rangle] = (4+a)[\langle K^- n | K^- n \rangle - \langle K^+ n | K^+ n \rangle], \quad (\text{B24})$$

$$2(1+a)[\langle K^- p | K^- p \rangle - \langle K^+ p | K^+ p \rangle] = (4+a)[\langle \pi^- p | \pi^- p \rangle - \langle \pi^+ p | \pi^+ p \rangle], \quad (\text{B25})$$

$$(2-a)[\langle \pi^- n | \pi^- n \rangle - \langle K^- n | K^- n \rangle] = (4+a)[\langle \pi^- p | \pi^- p \rangle - \langle K^- p | K^- p \rangle], \quad (\text{B26})$$

$$\langle \eta Y_1^{*-} | K^- n \rangle = \sqrt{2} \langle \eta Y_1^{*0} | K^- p \rangle, \quad (\text{B27}) \quad = \langle K^+ \Delta^0 | K^+ n \rangle \quad (\text{B42})$$

$$\langle \eta \Delta^{++} | \pi^+ p \rangle = -\sqrt{3} \langle \eta \Delta^0 | \pi^- p \rangle \quad (\text{B28}) \quad = -\langle K^0 \Delta^+ | K^+ n \rangle \quad (\text{B43})$$

$$= -\langle \eta \Delta^- | \pi^- n \rangle \quad (\text{B29}) \quad = -\sqrt{2} \langle \pi^- Y_1^{*0} | K^- n \rangle / b \quad (\text{B44})$$

$$= -(1/\sqrt{2}) [\langle K^+ \Delta^+ | K^+ p \rangle + \langle K^- \Delta^+ | K^- p \rangle], \quad (\text{B30}) \quad = \sqrt{2} \langle \pi^0 Y_1^{*-} | K^- n \rangle / b, \quad (\text{B45})$$

$$\sqrt{2} \langle \pi^0 \Delta^0 | \pi^- p \rangle = -\langle \pi^- \Delta^+ | \pi^- p \rangle \quad (\text{B31}) \quad = -b \langle K^- \Delta^+ | K^- p \rangle \quad (\text{B47})$$

$$= \langle \pi^+ \Delta^+ | \pi^+ p \rangle \quad (\text{B32}) \quad = -b \langle \bar{K}^0 \Delta^0 | K^- p \rangle \quad (\text{B48})$$

$$= (\frac{2}{3})^{1/2} \langle \pi^0 \Delta^{++} | \pi^+ p \rangle \quad (\text{B33}) \quad = \sqrt{2} \langle K^+ Y_1^{*0} | \pi^+ n \rangle \quad (\text{B49})$$

$$= \langle \pi^+ \Delta^0 | \pi^+ n \rangle \quad (\text{B34}) \quad = -\langle K^0 Y_1^{*-} | \pi^- n \rangle \quad (\text{B50})$$

$$= \sqrt{2} \langle \pi^0 \Delta^+ | \pi^+ n \rangle \quad (\text{B35}) \quad = -b \langle K^- \Delta^0 | K^- n \rangle \quad (\text{B51})$$

$$= -\langle \pi^- \Delta^0 | \pi^- n \rangle \quad (\text{B36}) \quad = -b \langle \bar{K}^0 \Delta^- | K^- n \rangle / \sqrt{3} \quad (\text{B52})$$

$$= (\frac{2}{3})^{1/2} \langle \pi^0 \Delta^- | \pi^- n \rangle \quad (\text{B37}) \quad = \frac{1}{2} [\langle \pi^- Y_1^{*+} | K^- p \rangle + \sqrt{6} \langle \eta Y_1^{*-} | K^- n \rangle], \quad (\text{B53})$$

$$= \langle K^+ \Delta^+ | K^+ p \rangle - \langle K^- \Delta^+ | K^- p \rangle, \quad (\text{B38}) \quad \langle \pi^- Y_0^* | K^- n \rangle = \sqrt{2} \langle \pi^0 Y_0^* | K^- p \rangle, \quad (\text{B54})$$

$$\langle K^+ \Delta^+ | K^+ p \rangle = -\langle K^0 \Delta^{++} | K^+ p \rangle / \sqrt{3} \quad (\text{B39}) \quad \langle K^0 Y_0^* | \pi^- p \rangle = \langle K^+ Y_0^* | \pi^+ n \rangle, \quad (\text{B55})$$

$$= -\langle \pi^- Y_1^{*+} | K^- p \rangle / b \quad (\text{B40}) \quad \sqrt{3} \langle \eta Y_0^* | K^- p \rangle = \langle \pi^0 Y_0^* | K^- p \rangle - \sqrt{2} \langle K^0 Y_0^* | \pi^- p \rangle. \quad (\text{B56})$$

$$= 2 \langle \pi^0 Y_1^{*0} | K^- p \rangle / b \quad (\text{B41})$$

¹Ramesh Chand, Phys. Lett. 26B, 535 (1968).

²V. Barger and L. Durand, Phys. Rev. 156, 1525 (1967).

³Compilation of Cross Sections, CERN/HERA Reports No. 72-1, and No. 72-2, 1972 (unpublished).

⁴H. Lipkin, in *Proceedings of the Heidelberg International Conference on Elementary Particles, 1967*, edited by H. Filthuth (North-Holland, Amsterdam, 1968), p. 253; E. Lohrmann, in *Proceedings of the Lund International Conference on Elementary Particles, 1969*, edited by G. von Dardel (Institute of Physics, Lund, Sweden, 1969), p. 11; N. Gelfand, in *Symposium on Nucleon-Antinucleon Interactions* (Argonne National Laboratory, Illinois, 1968), p. 4.

⁵H. Lipkin, Phys. Rev. Lett. 16, 1015 (1966); G. Joshi, V. Bhasin, and A. N. Mitra, Phys. Rev. 156, 1572 (1967); K. Johnson and S. B. Treiman, Phys. Rev. Lett. 14, 189 (1965).

⁶Ramesh Chand, Phys. Rev. D 2, 1955 (1970); 3, 1165 (1971).

⁷Ramesh Chand and A. Sundaram, Phys. Rev. D 2, 1952 (1970); Ramesh Chand, Prog. Theor. Phys. 44, 758 (1970).

⁸Ramesh Chand, Part. Nucl. 3, 69 (1972); 3, 183 (1972).

⁹S. Okubo, University of Rochester report (unpublished).

¹⁰Ramesh Chand and A. M. Gleeson, Part. Nucl. 1, 485 (1971).

¹¹S. Okubo and R. E. Marshak, Nuovo Cimento 28, 56 (1963).

¹²Ph. Salin, Nucl. Phys. B3, 323 (1967).

¹³V. Barger and M. Olsson, Phys. Rev. 146, 1080 (1966).

¹⁴S. Meshkov, G. Snow, and G. Yodh, Phys. Rev. Lett. 12, 87 (1964).

¹⁵M. Courdin, *Unitary Symmetries* (North-Holland, Amsterdam, 1967), p. 63.

¹⁶Ramesh Chand, Prog. Theor. Phys. 46, 492 (1971).

¹⁷N. Cabibbo, L. Horwitz, and Y. Ne'eman, Phys. Lett. 22, 366 (1966).

¹⁸Ramesh Chand, Part. Nucl. 3, 53 (1972).